Information Transfer in the Penta-EF-hand Protein Sorcin Does Not Operate via the Canonical Structural/Functional Pairing

A STUDY WITH SITE-SPECIFIC MUTANTS*

Manuela Mella, Gianni Colotti, Carlotta Zamparelli, Daniela Verzili, Andrea Ilari, and Emilia Chiancone‡

From the Consiglio Nazionale delle Ricerche Institute of Molecular Biology and Pathology, Department of Biochemical Sciences A. Rossi Fanelli, University of Rome La Sapienza, 00185 Rome, Italy

Sorcin is a typical penta-EF-hand protein that participates in Ca^{2+}-regulated processes by translocating reversibly from cytosol to membranes, where it interacts with different target proteins in different tissues. Binding of two Ca^{2+}/monomer triggers translocation, although EF1, EF2, and EF3 are potentially able to bind calcium at micromolar concentrations. To identify the functional pair, the conserved bidentate -Z glutamate in these EF-hands was mutated to yield E53Q-, E94A-, and E124A-sorcin, respectively. Limited structural perturbations occur only in E124A-sorcin due to involvement of Glu-124 in a network of interactions that comprise the long D helix connecting EF3 to EF2. The overall affinity for Ca^{2+} and for two sorcin targets, annexin VII and the ryanodine receptor, follows the order wild-type > E53Q- > E94A- > E124A-sorcin, indicating that disruption of EF3 has the largest functional impact and that disruption of EF2 and EF1 has progressively smaller effects. Based on this experimental evidence, EF3 and EF2, which are not paired in the canonical manner, are the functional EF-hands. Sorcin is proposed to be activated upon Ca^{2+} binding to EF3 and transmission of the conformational change at Glu-124 via the D helix to EF2 and from there to EF1 via the canonical structural/functional pairing. This mechanism may be applicable to all penta-EF-hand proteins.

Sorcin is a member of the penta EF-hand (PEF)[1] family, a small group of Ca^{2+} binding proteins that comprises the large and small calpain subunits (1, 2), grancalcin (3), ALG-2 (4), and peflin (5). All these proteins bind to cell membranes through a Ca^{2+}-dependent interaction with protein targets that permits transduction of various Ca^{2+}-mediated signals. Sorcin is thought to participate in different Ca^{2+}-triggered biochemical cascades since different target proteins have been identified in the cell types where the protein is expressed constitutively, namely the ryanodine receptor (Ryr) and the α_1 subunit of L-type calcium channels in muscle cells (6, 7), presenilin 2 in human brain (8), and annexin VII in adrenal medulla (9), differentiating myocytes (10) and red blood cells (11).

The EF-hand, a structural motif characterized by a helix-loop-helix structure, is used by a large number of proteins to bind Ca^{2+} with high affinity. In the "canonical" motif, Ca^{2+} is coordinated by a 12-amino-acid-long interhelical loop sequence with pentagonal bipyramidal symmetry. In this arrangement, four conserved side chains provide the five equatorial ligands (Y, Z, -Y, -Z) since the glutamate residue in position -Z establishes a bidentate interaction with the metal. The two apical ligands are furnished by the side chain of an acidic group (X) and by a water molecule (-X). Changes in the loop sequence occur such that the EF-hands may not bind Ca^{2+} or may not be recognized in the protein primary structure. In the PEF family, the extensively modified EF4 and EF5 loops do not bind Ca^{2+}, and the N-terminal motif designated EF1 was not recognized by sequence analysis since the loop is one amino acid shorter than the canonical one. The existence of the EF1 hand was revealed only by the x-ray crystal structure of the calpain subunits, the family prototype (1, 2).

In a typical manner, EF-hands occur in pairs that are coupled structurally and functionally. The structural association takes place through a short two-stranded β sheet arrangement that gives rise to stable domains. Moreover, binding of Ca^{2+} elicits a change from a "closed" to an "open" conformation that leads to exposure of hydrophobic surfaces for target interaction. In the PEF family, all the EF-hands are clustered in the C-terminal domain that is characterized by a very similar, compact fold in all the proteins, as exemplified by the sorcin structure depicted in Fig. 1. The EF1-EF2 and EF3-EF4 pairs are associated in the canonical manner, although EF5 is unpaired in the monomer but interacts with the same motif of a second monomer in the native form of the molecule, a dimeric assemblage (2, 12–14). An intriguing peculiarity of the Ca^{2+} binding domain is the unusual presence of two long (six turns) α-helices that are shared by EF2 and EF3 (D helix) and by EF4 and EF5 (G helix). At least in principle, this direct structural link between the two canonical EF-hand pairs may represent the natural means for transferring functional information between them. The compact structure of the C-terminal Ca^{2+} binding domain contrasts the flexibility of the N-terminal domain, which is of variable length in the different PEF proteins but is always rich in glycine and proline residues. Because of its nature, the N-terminal domain is not visible in the available x-ray crystal structures of the whole proteins, namely those of sorcin (15), grancalcin (13, 16), and calpain (17, 18).

[1] The abbreviations used are: PEF, penta EF-hand; Ryr, ryanodine receptor; PVDF, polyvinylidene difluoride; SPR, surface plasmon resonance; RU, resonance units.

The present understanding of the relationships between structure and function in the PEF family is far from complete. The x-ray structures show that three EF sites are potentially able to bind Ca^{2+} in the physiological range of concentrations, namely the unusual EF1 motif and EF2 and EF3, whose structural features resemble those of EF-hands in regulatory Ca^{2+}-binding proteins. However, binding of only two Ca^{2+}/monomer suffices to trigger the conformational change that exposes hydrophobic regions and leads to interaction with the respective targets (3, 19, 20). The available data indicate that functional coupling does not involve the same EF-hands in the different proteins, suggesting that despite the high structural similarity there is no common mode of information transfer within the PEF family. Furthermore, the mechanism of communication between Ca^{2+}-binding sites has not been elucidated. In sorcin, the characterization of a protein fragment (90–198) lacking the first two EF-hands pointed to EF1 and EF2 as the physiological pair (19). In grancalcin, EF1 and EF3 that are not linked structurally are coupled functionally; EF2 is unable to bind Ca^{2+} due to the presence of alanine in place of the canonical, bidentate -Z glutamate (3). In ALG-2, studies with site-specific mutants indicate that, as in grancalcin, the EF1 and EF3 motifs form the functionally relevant Ca^{2+} binding pair (4), whereas in calpain all the first three EF hands contribute to Ca^{2+} binding, with EF3 having the highest affinity (2).

The molecular mechanism that triggers the Ca^{2+}-signaling process and leads to a change in the subcellular localization of PEF proteins through the specific interaction with protein targets is still obscure. The Ca^{2+}-induced conformational changes manifest in the x-ray crystal structures are unexpectedly small and are limited to the EF1 region (1, 2, 13, 17), and it is not known how these small changes are amplified to the extent required for target protein interaction.

In the present work sorcin was used to address these aspects of the structure-function relationships in PEF proteins. Sorcin and its isolated Ca^{2+} binding domain have been characterized extensively in solution (19, 21–23). Moreover, a model for the Ca^{2+}-dependent processes in the full-length protein has been proposed on the basis of the x-ray crystal structure of the Ca^{2+} binding domain (12). Ca^{2+} binding is thought to weaken the interactions between the N- and C-terminal domains, thereby permitting their reorientation, which in turn facilitates interaction with the target proteins at or near membranes. It is relevant in this connection that sorcin has the ability to interact with its partners by means of both the N- and C-terminal domain, as exemplified by annexin VII and the ryanodine receptor, respectively (23, 19).

Site-specific mutants of EF1, EF2, and EF3 have been designed in which the canonical glutamate in the -Z position was changed into Gln or Ala. The respective mutant proteins, E53Q, E94A, E124A, have been characterized by determining their structural properties in solution and their affinity for Ca^{2+}. Thereafter, the effect of the site-specific mutation on the capacity to interact with annexin VII and the ryanodine receptor was assessed. Substitution of the -Z glutamate in the first three EF-hands produces structural alterations of very limited extent. They can be appreciated only in the E124A mutant due to the involvement of Glu-124 in a network of hydrogen bonding and hydrophobic interactions that comprise the D helix. All the substitutions introduced affect the Ca^{2+} binding properties of sorcin. The effect is largest when EF3 is modified and decreases in the order EF2 and EF1. These findings indicate that EF3 and EF2 represent the functional pair and suggest that binding of Ca^{2+} to EF3 is the first step in sorcin activation. It is conceivable that Ca^{2+} binding at the EF3 site changes the conformation of Glu-124 and that this change is transmitted to

EF2 via the long D helix. The subsequent step in the pathway could occur in the conventional manner by taking advantage of the canonical structural coupling between EF2 and EF1. This unusual mode of functional linkage may be operative in all PEF proteins given their high structural similarity and, hence, may represent a general property of the family.

MATERIALS AND METHODS

Cloning of Sorcin Mutants—The cDNA of Chinese hamster ovary sorcin, kindly provided by Dr. M. B. Meyers, was amplified by PCR using two oligonucleotides, one of which was designed to generate a novel *Nde*I restriction site at the 5′ end at the place of *Nco*I without altering the sequence within the gene. The amplified DNA thus obtained was digested with the restriction enzymes *Nde*I and *Hin*dIII and was inserted subsequently in a pET22 expression vector (Novagen, Madison, WI) that had been digested with the same enzymes. Site-directed mutagenesis was carried out by the PCR overlap extension mutagenesis method according to Higuchi *et al.* (24) using the proofreading enzyme *Pfu* DNA polymerase to avoid the addition of 3′-overhanging residues by *Taq* polymerase. The following oligonucleotides were used: N forward, 5′-GCGAAATTAATACGACTCACTATAGGG-3′; C reverse, 5′-CAAGCTTTTAGACGGTCATGACAC-3′; E53Q forward, 5′-CAAATTGATGCTGATCAGTTGCAGAGATGTCTAAC-3′; E53Q reverse, 5′-GTTAGACATCTCTGCAACTGATCAGCATCAATTTG-3′; E94A forward, 5′-CACCATGGGATTCAATGCATTTAAAGAGCTC-3′; E94A reverse: 5′-GAGCTCTTTAAATGCATTGAATCCCATGGTG-3′; E124A forward, 5′-GGAACGGTGGATCCCCAGGCACTGCAGAAG-GCTCTG-3′; E124A reverse, 5′-CGTCAGAGCCTTCTGCAGTGCCTG-GGGATCCACCGT-3′. The complete mutated genes were digested with *Nde*I and *Hin*dIII and cloned into a pET22 expression vector.

Expression and Purification of Wild-type Sorcin and Its Mutants—Chinese hamster ovary recombinant sorcin was expressed in *Escherichia coli* BL21 (DE3) cells and was purified as previously described (21). The protein concentration was determined spectrophotometrically at 280 nm using a molar extinction coefficient on a monomer basis of 29,400 (21). The same purification procedure and the same extinction coefficient were used for the mutant proteins.

Circular Dichroism Spectra—CD spectra were recorded on a Jasco J-710 spectropolarimeter in the far UV (195–240 nm) and in the near UV (250–350 nm) region. The experiments at pH 7.5 were carried out at 20 °C in 5 mM Tris-HCl buffer, and those at pH 6.0 were carried out in 0.1 M sodium acetate buffer at 40 °C. The α-helical content was calculated from the ellipticity value at 222 nm according to Chou and Fasman (25).

Determination of Ca^{2+} Affinity—Indirect titrations were carried out in a Fluoromax spectrofluorimeter in 0.1 M Tris-HCl buffer at pH 7.5 and 25 °C in the presence of the fluorescent calcium chelator Quin2, according to Bryant (26). The excitation wavelength was 339 nm (slit width, 0.5 nm); the increment of emission intensity due to calcium binding to Quin2 was followed at 492 nm. Special care was taken to reduce Ca^{2+} contamination to 0.5–1.0 μM by treating the protein solutions and the glassware with Chelex 100, as recommended by André and Linse (27). For each mutant four sets of independent experiments were carried out, which included control titrations of Quin2 alone and of native sorcin. At the end of each titration, the fluorescence intensity corresponding to zero free Ca^{2+} concentration was determined by the addition of 5 mM EGTA. The fluorescence intensity of Quin2 at high calcium concentrations was taken as the higher asymptote. To estimate the Ca^{2+} affinity constants of native sorcin and its mutants, each experimental set was fitted with the program CaLigator (27); the choice between one and two binding constants was made on the basis of the χ^2 values.

Interaction of Wild-type Sorcin and Its Mutants with Annexin VII in Overlay Assay Experiments—Aliquots of purified wild-type sorcin and of the mutants were subjected to electrophoresis on a 15% polyacrylamide gel under denaturing conditions (28) and transferred to polyvinyl difluoride membranes (PVDF, Problott, Applied Biosystems, Foster City, CA) in transfer buffer (25 mM Tris-HCl, 192 mM glycine, 20% methanol, pH 8.3) for 45 min at 100 mA (29). For Western blotting analysis, the PVDF membranes were incubated at room temperature with annexin VII (5 μg/ml) in 1% gelatin in TBST buffer (20 mM Tris-HCl, 0.5 M NaCl, 0.05% Tween 20, pH 7.5) containing 10 μM or 500 μM $CaCl_2$. Subsequently, the membranes were incubated with anti-annexin VII polyclonal antibody (dilution 1:3000) in 1% gelatin in TBST buffer. The blots were developed by incubation with alkaline phosphatase conjugate monoclonal anti-mouse IgG (Sigma) in 1% gelatin in TBST. Control experiments ruled out the existence of cross-reactivity
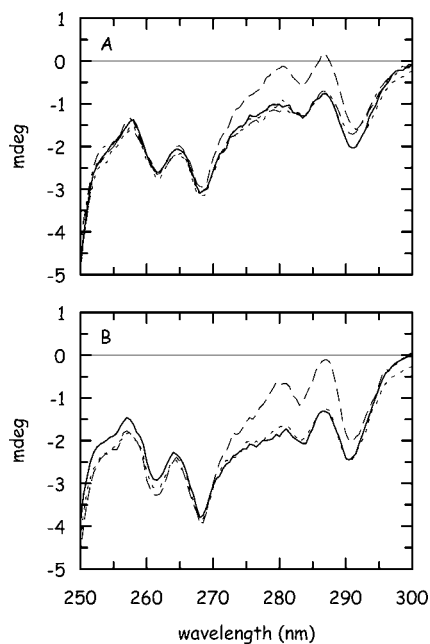
between sorcin and its mutants and the anti-annexin VII antibody (data not shown).

Interaction of Wild-type Sorcin and Its Mutants with Annexin VII in Surface Plasmon Resonance (SPR) Measurements—SPR experiments were carried out using a BIACORE X system (Biacore AB, Uppsala, Sweden). Two N-terminal peptides of annexin VII were synthesized by Sigma-Genosys (Cambridge, UK); to improve the peptide solubility and binding to the sensor chip, three lysine residues were added to the first 20 amino acids of annexin VII (MSYPGYPPTGYPPFPGYPPA). Peptide P1 contained three lysine residues at the N terminus of the sequence, whereas peptide P2 contained three lysine residues at the C-terminal end. The peptide purity was checked by matrix-assisted laser desorption ionization time-of-flight mass spectrometry. The calculated isoelectric point of both P1 and P2 is 9.90, based on the program pI-tool (30).

The sensor chips (CM5, Biacore AB) were activated chemically by injection of 35 μl of a 1:1 mixture of *N*-hydroxysuccinimide (50 mM) and *N*-ethyl-*N'*-(3-dimethylaminopropyl)carbodiimide (200 mM) at a flow rate of 5 μl/min. The N-terminal peptides of annexin VII were immobilized on the activated sensor chip via amine coupling. The reaction was carried out in 20 mM sodium acetate at pH 6.0, and the remaining ester groups were blocked by injecting 1 M ethanolamine hydrochloride (35 μl). In control experiments, the sensor chip was treated as described above in the absence of peptide. The interaction of the immobilized annexin VII peptides with wild-type sorcin and its mutants was detected through mass concentration-dependent changes of the refractive index on the sensor chip surface. The changes in the observed SPR signal are expressed as resonance units (RU). Typically, a response change of 1000 RU corresponds to a change in the surface concentration on the sensor chip of about 1 ng of protein per mm^2 (40). The experiments were carried out at 25 °C in 10 mM HEPES, pH 7.4, 0.15 M NaCl, and 0.005% surfactant P-20 (HBS-P buffer), treated with Chelex 100 to eliminate contaminating calcium, and degassed. For the experiments as a function of Ca^{2+} concentration, calcium chloride or EGTA were added to the buffer. Measurements were performed at a flow rate of 20 μl/min with an immobilization level of the annexin VII N-terminal peptides corresponding to 200–1200 RU. Values of the plateau signal at steady state (R_{eq}) were calculated from kinetic evaluation of the sensorgrams using the BIAevaluation 3.0 software. Scatchard analysis of the dependence of R_{eq} on the concentration of wt sorcin was also performed to assess the equilibrium dissociation constant at 25 μM Ca^{2+}. The amine coupling kit, the surfactant P-20, and the CM-5 sensor chip were purchased from Biacore AB; all the other reagents were high purity grade.

Interaction of Wild-type Sorcin and Its Mutants with the Ryanodine Receptor—Aliquots of purified wild-type sorcin, EF1, EF2, and EF3 sorcin mutants were transferred to PVDF membranes as described above for the sorcin-annexin VII interaction. Incubation of the membranes with terminal cisternae vesicles from rabbit skeletal muscle enriched in Ryr (5 μg/ml) was likewise carried out in TBST buffer containing 10 μM or 500 μM CaCl$_2$ as described above. The blots were incubated with an anti-Ryr monoclonal antibody (INALCO) and were developed by incubation with alkaline phosphatase conjugate monoclonal anti-mouse IgG. Control experiments ruled out the existence of cross-reactivity between sorcin and its mutants and the anti-Ryr antibody (data not shown).

RESULTS

Structural Characterization of the Site-specific Sorcin Mutants—Far and near UV CD spectroscopy was used to assess the possible occurrence of structural changes in the mutated apoproteins. The experiments were carried out at pH 7.5 and at pH 6.0 since the x-ray crystal structure of the Ca^{2+} binding domain was obtained at the latter pH value (12). Although sorcin operates in a medium containing about 1 mM Mg^{2+}, this cation was not included in the buffers used throughout this study since previous work showed that Mg^{2+} has no effect on the structural and functional properties of the protein (21). The far UV CD spectra of all the site-specific mutants under study are indistinguishable from those of native sorcin both at pH 6.0 and at pH 7.5 (data not shown).

In the near UV CD region the spectrum of wild-type sorcin is negative and is characterized by two sharp bands at 262 and 268 nm attributed to phenylalanines, by a weaker band at 283 nm due to the tyrosyl fine structure (0–0 transition), and by a fairly intense, well resolved peak at 292 nm due to tryptophan residues (22). The two tryptophan residues, Trp-99 and Trp-

FIG. 1. **Structure of sorcin.** *A*, amino acid sequence. The residues conserved in all members of the PEF family are in *bold*; the residues in the Ca^{2+}-coordinating positions are in *gray*. *B*, x-ray structure of the sorcin Ca^{2+} binding domain (Protein Data Bank code 1GJY; Ref. 12). *C*, blow-up of the D helix (*pale blue*) and of the structural elements that take part in the proposed signal transduction mechanism. The residues involved in hydrogen bonding (Tyr-67–Asp-113, Glu-124–Phe-112) are in *red*, and those forming the hydrophobic core (Phe-70, Trp-99, Trp-105, Tyr-159) around the D helix are in *yellow*. The EF-hands (EF1-EF3) are also indicated. The picture is depicted in MOLSCRIPT (39).

105, which are located on the D helix (Fig. 1, *B* and *C*), both contribute to the observed signal. However, the contribution of Trp-99 is likely to be smaller since this residue is more exposed to solvent than Trp-105 (12). The spectra of the mutant proteins are very similar to those of wild-type sorcin at both pH values with the exception of E124A, albeit only over the wavelength range 272–300 nm (Fig. 2). Thus, in the E124A mutant, the phenylalanine bands are unchanged, whereas the bands of

FIG. 2. **Near UV circular dichroism spectra of wild-type sorcin and of the E53Q, E94A, and E124A mutants.** Wild-type sorcin (——), E53Q (········), E94A (—), and E124A (– –) were at a concentration of 50 μM. *A*, 0.1 M sodium acetate buffer, pH 6.0, 40 °C. *B*, 0.1 M Tris-HCl buffer, pH 7.5, 25 °C.
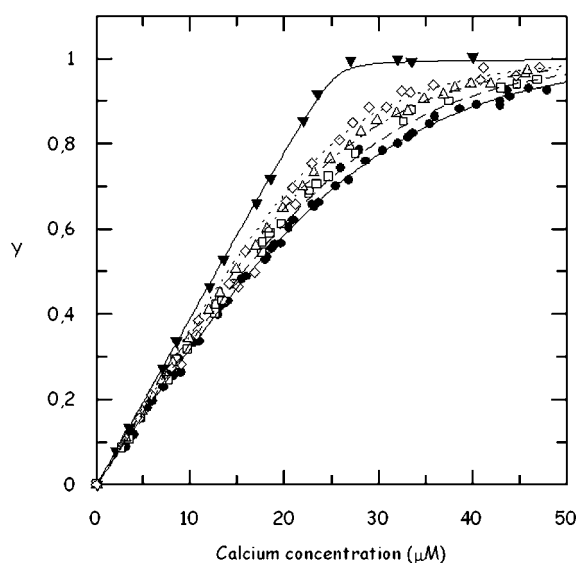

FIG. 3. **Fluorescence titration of wild-type sorcin and of the E53Q, E94A, and E124A mutants with calcium in the presence of the calcium chelator Quin2.** The degree of saturation of Quin2 (*y*) is plotted as a function of total calcium concentration. Wild-type sorcin (●), E53Q (□), E94A (△), and E124A (◇) at a concentration of 25 μM were titrated with calcium in the presence of 25 μM Quin2 in 0.1 M Tris-HCl at pH 7.5 and 25 °C. The titration of Quin2 alone (▼) is also shown. Four sets of independent titrations were carried out for native sorcin and for each mutant.

tyrosine and tryptophan residues occur at the same wavelength as in the wild-type protein at both pH values but have a smaller amplitude. The difference is particularly significant for the tyrosine contribution.

Sorcin precipitates upon binding of 2 Ca^{2+}/monomer in the absence of target proteins due to the exposure of hydrophobic surfaces (22). The same phenomenon was observed also for the site-specific mutants under study. Therefore, the effect of calcium on the near UV CD spectra was not studied.

Calcium Affinity of the Site-specific Sorcin Mutants—As for the wild-type protein (19), the affinity for calcium could not be determined in direct fluorescence experiments since the fluorescence intensity is practically unchanged upon binding of 2 eq of Ca^{2+}/monomer, and higher amounts of calcium lead to precipitation.

Calcium affinity was assessed in indirect fluorescence titration experiments in the presence of the calcium chelator Quin2. The results obtained at pH 7.5 are presented in Fig. 3 in terms of the degree of saturation of Quin2 as a function of total calcium concentration. Simple inspection of the data indicates that in the mutants calcium affinity decreases with respect to the wild-type protein in the order E53Q > E94A > E124A.

An important consequence of the occurrence of precipitation upon saturation of sorcin with 2 eq of Ca^{2+}/monomer is that higher Ca^{2+}/protein ratios cannot be scrutinized. Hence, one cannot establish whether more than two high affinity Ca^{2+}-binding sites are present on the sorcin molecule and is forced to analyze the titration data in terms of a two-site model. In the framework of this minimum scheme and on the basis of the statistical parameters obtained from the fitting procedure, the behavior of the wild-type protein can be described with two apparent dissociation constants in the micromolar range, namely $K_1 = 0.42 \pm 0.05 \times 10^{-6}$ M and $K_2 = 6.3 \pm 4.1 \times 10^{-6}$ M, using a dissociation constant for the chelator of 60 nM at pH 7.4, 20 °C (31). On the other hand the binding profiles of the mutants can be fitted satisfactorily by a single binding constant corresponding to $0.48 \pm 0.13 \times 10^{-6}$ M in E53Q, $0.71 \pm 0.14 \times 10^{-6}$ M in E94A, and $1.10 \pm 0.27 \times 10^{-6}$ M in E124A. For the

mutants the second constant cannot be determined with accuracy because it is below the resolution limits of the technique under the experimental conditions used (about 1×10^{-5} M).

If one assumes that the site-specific mutations studied introduce local structural perturbations, the observed changes in Ca^{2+} affinity can be taken to indicate that glutamic acid in the -Z position of the EF3 hand is more important than the corresponding residue of the EF2 and of the EF1 hands in determining the Ca^{2+}-dependent conformational change that permits interaction with the target proteins. To prove this contention, binding of the mutant proteins with two physiological sorcin partners was assessed, namely annexin VII and Ryr, which are known to interact with the N- and C-terminal sorcin domains, respectively (23, 19).

Interaction of Wild-type Sorcin and Its Site-specific Mutants with Annexin VII and the Ryanodine Receptor in Immunoblot Experiments—In a first set of experiments wild-type sorcin and its mutants were transferred to PVDF membranes and incubated with annexin VII at pH 7.5 in buffer containing 10 or 500 μM calcium. Polyclonal anti-annexin VII antisera were used to detect complex formation. At the lower calcium concentration, wild-type sorcin and the E53Q and the E94A mutant appear to interact similarly with annexin VII, whereas no interaction occurs in the case of the E124A mutant. At the higher calcium concentration (500 μM) all the proteins interact with annexin VII in a similar manner (Fig. 4).

A second set of experiments was carried out to test the interaction with Ryr under the same experimental conditions. Wild-type sorcin and its mutants were blotted on PVDF membranes and incubated with Ryr-enriched terminal cisternae vesicles from rabbit skeletal muscle, and monoclonal anti-Ryr antibodies were used to detect complex formation. In accordance with the results obtained with annexin VII, at about 10 μM calcium native sorcin, the E53Q and the E94A mutants form a complex with the ryanodine receptor, whereas no interaction occurs in the case of E124A. At the higher calcium concentration, sorcin and the mutants all interact to a similar extent with Ryr (Fig. 5). It should be mentioned that no inter-
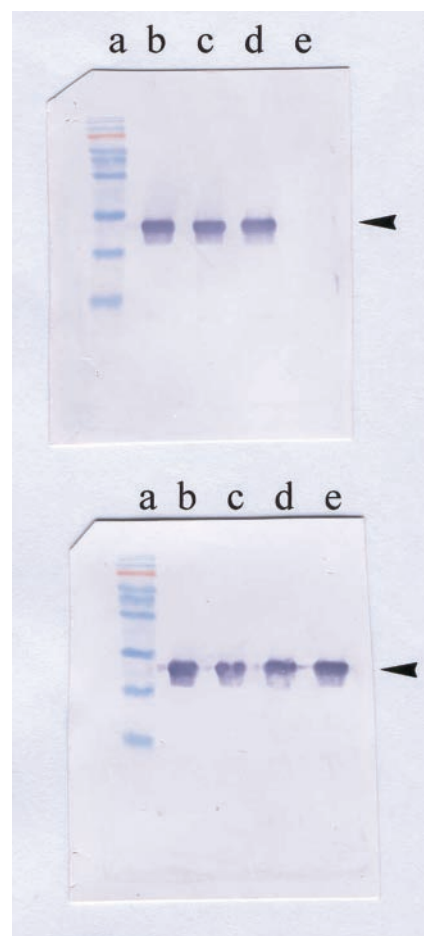
FIG. 4. **Interaction of wild-type sorcin and of the E53Q, E94A, and E124A mutants with annexin VII in the presence of 10 μM (*upper panel*) or 500 μM CaCl$_2$ (*lower panel*).** *a*, molecular weight markers (180, 130, 100, 73, 54, 50, 35, 24, 16, and 10 kDa). *b*, wild-type sorcin; *c*, E53Q; *d*, E94A; *e*, E124A subjected to SDS-PAGE (28) and transferred to PVDF membranes (29). The PVDF membranes were incubated with annexin VII in buffer containing 10 μM (*upper panel*) or 500 μM CaCl$_2$ (*lower panel*) and subsequently with anti-annexin VII polyclonal antibody. The *arrows* indicate the band corresponding to sorcin (M_r 21.5 kDa).

FIG. 5. **Interaction of wild-type sorcin and of the E53Q, E94A, and E124A mutants with the ryanodine receptor in the presence of 10 μM (*upper panel*) or 500 μM CaCl$_2$ (*lower panel*).** *a*, molecular weight markers (180, 130, 100, 73, 54, 50, 35, 24, 16, and 10 kDa); *b*, wild-type sorcin; *c*, E53Q; *d*, E94A; *e*, E124A subjected to SDS-PAGE (28) and transferred to PVDF membranes (29). The PVDF membranes were incubated with terminal cisternae vesicles from rabbit skeletal muscle enriched in ryanodine receptor in buffer containing 10 μM (*upper panel*) or 500 μM CaCl$_2$ (*lower panel*) and subsequently with anti-Ryr monoclonal antibody. The *arrows* indicate the band corresponding to sorcin (M_r 21.5 kDa).

action of sorcin and its mutants with annexin VII or with Ryr was observed in control experiments carried out in EGTA-containing buffer (data not shown).

Interaction of Wild-type Sorcin and Its Site-specific Mutants with the N-terminal Peptide of Annexin VII in SPR Experiments—SPR was used to obtain quantitative information on the interaction between sorcin and annexin VII, which is known to involve the N-terminal domains of both proteins (9, 23).

During the course of previous experiments, the lifetime of chips with immobilized annexin VII was found to be limited to a few days (23). To increase the chip stability, the use of a synthetic peptide corresponding to the annexin VII N terminus (amino acids 1–20) was explored. The use of the annexin N terminus has a further advantage. Because this peptide does not bind Ca^{2+}, a simplified experimental picture is obtained by annulling the contribution of Ca^{2+} binding to the target protein. The peptide was rendered soluble by introducing three lysine residues before amino acid 1 (peptide P1) or at the end of the sequence (peptide P2). Both P1 and P2 are immobilized efficiently on CM5 chips and react similarly with wild-type sorcin in the presence of calcium at micromolar concentrations, although P1 yields consistently higher RU values. Like immobilized full-length annexin VII (23), the immobilized peptides

regain full binding activity after treatment with EGTA-containing buffer, which leads to complete dissociation of bound sorcin. Verzili *et al.* (23) established that at pH 7.5 and 6 μM calcium the interaction of immobilized full-length annexin VII with sorcin is significant ($K_D = 0.63$ μM). Under similar conditions, the immobilized P1 peptide yields apparent K_D values in the order of 1 μM, in good agreement with the results obtained with the full-length protein. The P1 peptide, therefore, was chosen for the systematic study of the interaction with sorcin and its mutants.

The Ca^{2+} dependence of the interaction with the N-terminal peptide of annexin VII was assessed at constant (300 nM) concentration of native or mutant sorcin. Typically, the sensorgrams display three phases (Fig. 6); the initial increase in RU from the base line corresponds to association of sorcin or its mutants to the immobilized annexin peptide, the plateau region represents the steady-state phase of the interaction, where the rate of sorcin association to the immobilized peptide is balanced by the rate of its dissociation from the complex, and the decrease in RU corresponds to the dissociation phase during buffer flow at the end of the sample injection. Simple inspection of the sensorgrams depicted in Fig. 6, *A–D*, shows that in the mutants both k_{on} and k_{off} increase with respect to
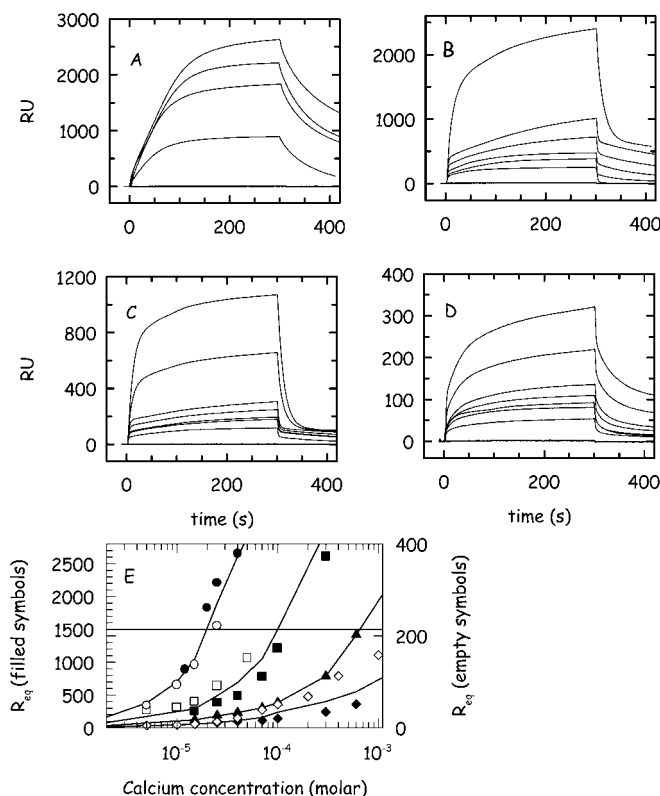
FIG. 6. **SPR experiments on the binding of sorcin or its E53Q, E94A, and E124A mutants to the immobilized N-terminal peptide of annexin VII as a function of calcium concentration.** In the sensorgrams (*A–D*) wild-type sorcin or its mutants at a concentration of 300 nM were injected at time 0 onto the chip containing the immobilized N-terminal annexin VII peptide. The increase in RU relative to the base line indicates complex formation; the plateau represents the steady-state phase of the interaction, whereas the decrease in RU represents the dissociation of sorcin from the immobilized annexin VII peptide attendant injection of buffer (10 mM HEPES, 0.15 M NaCl, 0.005% surfactant P20 at pH 7.4) at 25 °C. *A*, wild-type sorcin in buffer containing 2 mM EGTA and 12, 20, 25, and 40 μM CaCl$_2$ (from *bottom* to *top*). *B*, E53Q mutant in buffer containing 2 mM EGTA, 15, 25, 40, 70, 100, and 300 μM CaCl$_2$ (from *bottom* to *top*). *C*, E94A mutant in buffer containing 2 mM EGTA and 15, 25, 40, 70, 100, 300, and 600 μM CaCl$_2$ (from *bottom* to *top*). *D*, E124A mutant in buffer containing 2 mM EGTA and 15, 25, 40, 70, 100, 300, and 600 μM CaCl$_2$ (from *bottom* to *top*). *E*, the plateau signal at steady state (R_{eq}) is plotted as a function of total calcium concentration. Wild-type (● and ○), E53Q (■ and □), E94A (▲), and E124A (♦ and ◇) sorcin. *Filled* and *empty symbols* refer to data obtained with two different chips.

native sorcin, whereas the RU values in the plateau region and, hence, the amount of bound analyte decrease at any given calcium concentration. Moreover, for each protein the R_{eq} values increase when the calcium concentration in the medium increases. Fig. 6*E* summarizes the R_{eq} values obtained from the data depicted in Fig. 6, *A–D*, and in another independent set of experiments. The R_{eq} values show that the affinity for the annexin N terminus decreases in the order wt sorcin > E53Q > E94A > E124A.

A quantitative estimate of the equilibrium dissociation constant could be obtained only for wt sorcin by measuring the dependence of the R_{eq} values on sorcin concentration at constant Ca^{2+} (25 μM). Scatchard analysis of the data yielded an asymptotic value of about 3000 RU, corresponding to saturation of the immobilized annexin VII N-terminal peptide with wt sorcin, and an apparent K_D value of about 45 nM describing this interaction (data not shown). Under these experimental conditions, the R_{eq} values for the mutants are much lower than for wt sorcin, pointing to much higher dissociation equilibrium constants, such that the K_D values could not be assessed with

accuracy. However, if the same asymptotic value of 3000 RU is assumed for wt sorcin and its mutants, the data of Fig. 6*E* can be used to estimate the strength of the sorcin-annexin peptide interaction. In fact, the sorcin concentration that yields an R_{eq} value of 1500, *i.e.* 50% saturation of the immobilized annexin peptide, corresponds to the K_D value. The existence of a linkage between the immobilized peptide-sorcin equilibrium and the binding of Ca^{2+} demands that the lower the affinity of the sorcin mutant for the immobilized annexin VII peptide, the higher the Ca^{2+} concentration has to be to achieve the same R_{eq} value. On this basis, an apparent K_D of about 300 nM is obtained at about 18 μM Ca^{2+} for native sorcin and at increasingly higher Ca^{2+} concentrations for the EF1, EF2, and EF3 mutants, namely 100 μM for E53Q, 600 μM for E94A, and about 5 mM for E124A.

DISCUSSION

The present data provide insight into the molecular details of the events that start with the Ca^{2+} binding step, lead to activation of sorcin, and ultimately result in its interaction with protein targets at or near cell membranes. The behavior of the three site-specific sorcin mutants studied shows that the EF3 hand is the site endowed with the highest affinity for Ca^{2+}. Because the structurally associated EF4 site is defective and does not bind the metal, the typical EF-hand structural/functional pairing cannot operate (32). It is conceivable that information of Ca^{2+} binding to EF3 is transferred to the rest of the molecule by taking advantage of the specific hydrogen-bonding interactions established by the EF3 Ca^{2+} binding loop and of the long D helix that connects EF3 to EF2. The proposed mechanism may be applicable to all members of the PEF family since these structural properties are common to all these proteins.

In sorcin, only the first three EF-hands are potentially capable of binding Ca^{2+} at micromolar concentrations. In EF4, the loop is non-canonical (only 11 residues long), the metal-coordinating residue in position Y is lacking, and the bidentate -Z glutamic acid is substituted by the shorter aspartic acid. EF5 is likewise defective since the loop is two residues shorter than in canonical EF-hands and there is no glutamic acid in position -Z. A comparison of the sequences of EF1 through EF3 predicts that the EF3-hand should be endowed with the highest affinity for calcium due to the presence of four acidic residues in the metal coordination positions. Indeed, EF3 is the most conserved EF-hand within the PEF family in terms of Ca^{2+}-coordinating ligands (33). The unusual EF1 site has a gap in the Y coordination position and lacks an acidic residue at position X. In EF2, which is canonical in term of length and similar in sequence to EF3, the affinity for Ca^{2+} should be diminished relative to EF3 by the substitution of the canonical aspartate in position -X by a glycine residue. EF1 and EF2 are associated structurally through a canonical short two-stranded β sheet arrangement in which Met-90 and Gly-91 establish hydrogen bonds with Gln-48 and Ile-49, respectively. It is of interest that a methionine residue (Met-90) can take the place of the highly conserved isoleucine and valine residues in position 8 of the EF2 Ca^{2+} binding loop without disrupting the interaction with the partner EF1, at variance with observations on calmodulin mutants (34, 35). However, these sequence-based arguments do not allow one to predict how different the Ca^{2+} affinities of the first three sites will be.

To arrive at an experimental assessment of this property, the highly conserved glutamate at position -Z has been chosen for site-specific mutagenesis in the first three Ca^{2+} binding motifs, with the expectation that removal of the bidentate coordination with the metal would abolish the capacity of the mutated site to bind Ca^{2+}, as has been observed for site-specific m-calpain

mutants (36). Accordingly, the assumption made in the interpretation of the results is that any given mutation influences the structural and functional properties of the mutated site, leaving those of the other EF motifs essentially unaltered. It follows that only those mutations involving a physiologically relevant site are expected to alter the properties of the mutant significantly relative to the native protein.

The behavior of the site-specific mutants under study supports these ideas. The structural markers used, namely the far and near UV CD spectra, indicate that in the mutant proteins both the global fold of wild-type sorcin and the environment of the aromatic residues are essentially unperturbed. The only exception concerns the environment of tyrosine and tryptophan residues in the E124A mutant as manifest in the near UV CD spectrum. In particular the tyrosine band at 283 nm has a significantly smaller amplitude than in the native protein and in the E53Q and E94A mutants (Fig. 2). The observed change can be attributed to participation of the Glu-124 carboxylate in a network of hydrogen-bonding and hydrophobic interactions that reaches Tyr-67 located on the loop connecting EF1 to EF2. In Ca^{2+}-free sorcin the Glu-124 carboxylate is not solvent-exposed, as is usually the case for the -Z ligand in regulatory Ca^{2+}-binding proteins (12, 15), but is hydrogen-bonded to Phe-112, located at the D helix C terminus (Fig. 1*C*). This phenylalanine residue is part of an extended hydrophobic core that includes Phe-70, Phe-156, Phe-159, the two Trp residues (99 and 105) on the D helix, and the aromatic ring of Tyr-67. In turn, the Tyr-67 OH group is hydrogen bonded to Asp-113 (OD2), which occupies the X position in the EF3 Ca^{2+} binding loop. Tyr-67, due to this hydrogen-bonding interaction and to coupling with the electronic π-π^* transitions of the neighboring aromatic side chains, should contribute significantly to the strength of the tyrosine CD-band (37). If this holds true, disruption of the interaction network should result in a significant decrease of the band amplitude as is indeed observed in the E124A mutant. The concomitant decrease in the tryptophan band at 292 nm is of importance for its functional implications. It indicates that the loss of the hydrogen-bonding interactions established by Asp-113 and Glu-124 of the EF3 Ca^{2+} binding loop is sensed also by Trp-99 and Trp-105, located on the long and relatively rigid D helix that connects EF3 to EF2 (Fig. 1*C*). The D helix, therefore, appears capable of transmitting the structural perturbations originating in the EF3 Ca^{2+} binding loop far from the site of mutation. This role of the D helix is reminiscent of that played in calmodulin by the long Leu-69–Phe-92 E-helix that transmits the occurrence of Ca^{2+} binding between the two Ca^{2+} binding domains. In calmodulin, alteration of a single hydrogen bond, like that established between glutamic acid (Glu-82) of the E helix with Tyr-138, has the potential to disrupt the structural coupling between the two domains (38), as observed for the E124A sorcin mutant.

The changes in the near UV CD spectrum just discussed are observed uniquely in the E124A mutant (Fig. 2). This fact taken together with the far-reaching effects of the Glu-124 mutation, points to EF3 as the ideal trigger of the pathway that leads from Ca^{2+} binding to sorcin activation. A first, qualitative indication that this view is correct is provided by the close similarity of the near UV CD spectra measured in native sorcin (22) and the isolated Ca^{2+} binding domain (data not shown) during the first stages of Ca^{2+} titrations with that of the E124A mutant. It may be envisaged that in the native protein the first metal ion is coordinated by the EF3 Ca^{2+} binding loop with loss of the H-bonds established by Asp-113 and Glu-124 just as in the E124A mutant. There is, however, another requirement for this picture to be true, namely EF3 should be endowed with the highest affinity for Ca^{2+}. The fluorescence titration data in the presence of Quin2 show that it is so (Fig. 3). The overall affinity for Ca^{2+} follows the order wild-type sorcin > E53Q > E94A > E124A, indicating that disruption of the EF3 site has the largest effect on this property of the protein. Disruption of the EF2 and EF1 sites has progressively smaller effects.

Direct evidence for the major functional role of EF3 is provided by the immunoblot and SPR experiments, which allow a measure of the interaction with physiological targets and of its Ca^{2+} dependence. Based on the immunoblot data, the E124A mutant requires a significantly higher Ca^{2+} concentration (500 μM) than wild-type sorcin or the E53Q and E94A mutants (about 10 μM) for interaction with the binding partners. Figs. 4–5 show that there is no significant difference between annexin VII and Ryr, which interact with the N- and C-terminal sorcin domains, respectively (23, 19). Importantly, all the mutants retain the capacity to be activated by Ca^{2+}, in accordance with the fact that they are all able to translocate reversibly to *E. coli* membranes at millimolar concentrations of the cation, as observed during the purification procedure.

A better estimate of the Ca^{2+} concentration required to activate the mutants is furnished by the SPR experiments that involve measurement of their interaction with the immobilized N-terminal peptide of annexin VII. This peptide provides a suitable model to monitor complex formation between the whole protein and sorcin, as indicated by the data of Brownawell and Creutz (9) and by the control experiments performed. Fig. 6 shows that at any given Ca^{2+} concentration, the amount of complex formed decreases in the order wild-type sorcin > E53Q > E94A > E124A, which parallels their affinity for Ca^{2+} (Fig. 3). In wt sorcin an apparent K_D of 300 nM is obtained at about 18 μM Ca^{2+}. The E53Q, E94A, and E124A mutants require a 5-, 30-, and 250-fold increase in Ca^{2+} concentration, respectively, to interact with the immobilized annexin VII peptide with similar K_D values. It follows that sorcin activation at micromolar Ca^{2+} concentrations requires preservation not only of the EF3 but also of the EF2 hand. On this basis EF3 and EF2 can be identified as the physiological pair.

The picture that emerges is that EF3 is the major player in sorcin functionality. It has the highest affinity for Ca^{2+} and can trigger a Ca^{2+}-dependent conformational change by means of the hydrogen-bonding interactions established by Asp-113 and Glu-124 in the Ca^{2+} binding loop. The conformational change, although limited in extent, reaches EF2 and the EF1-EF2 loop through reorganization of the hydrophobic core packing around the D helix, which comprises Phe-95 and residues LWAVL in positions 98–102, Trp-105, Ile-110, Phe-112, Phe-156, and Phe-159. The canonical pairing of EF2 and EF1 facilitates transfer of information to the latter site. Integrity of the whole transmission pathway is necessary for sorcin activation, as shown by the behavior of the 90–198 sorcin fragment, which lacks EF1 and EF2. This fragment binds Ca^{2+} with decreased affinity and is unable to translocate to membranes, a finding that suggested wrongly that EF1 and EF2 represent the physiological pair (19).

The x-ray crystal structures of native sorcin and of the sorcin binding domain support the mechanism just proposed in that the different conformations predicted by the model of sorcin activation are frozen in individual monomers. This implies that the energies involved in the Ca^{2+}-induced rearrangements of the sorcin molecule are balanced by the lattice energies. In the structure of the whole molecule (15), the D helix and the loop connecting EF1 to EF2 have slightly different conformations in the two monomers forming the dimer. In one monomer Tyr-67 is hydrogen-bonded to Asp-113, and the D helix is rather straight, whereas in the other monomer the hydrogen bond is missing, the phenol moiety points toward the solvent, and the

D helix is slightly bent. In the structure of the sorcin Ca^{2+} binding domain (12), which has a tetramer in the asymmetric unit, monomers belonging to different dimers display relevant differences that are concentrated in the EF3 Ca^{2+} binding loop, in the D helix, and in the loop connecting EF3 to EF4. It is of interest that the EF3-EF4 loop interacts with the N-terminal peptide in the model proposed by Ilari *et al.* (12), which depicts the interaction between the C- and the N-terminal domains.

The very minor conformational changes that differentiate the x-ray crystal structures of the Ca^{2+}-free and Ca^{2+}-bound forms of calpain (1, 2) and grancalcin (3, 13) are likewise consistent with the mechanism proposed. The observed changes are limited to the EF1 region. This region is linked to the flexible N-terminal domain and, hence, must amplify the Ca^{2+}-induced conformational changes just described to bring about the exposure of hydrophobic residues for interaction with the binding partners. As a matter of fact, the mechanism proposed may be applicable to all members of the PEF family since they share the structural/functional elements necessary for sorcin activation. Thus, EF3 is the Ca^{2+}-binding site with the highest affinity for the metal, the -Z glutamate and Y aspartate residues in the EF3 Ca^{2+}-binding loop are not solvent-exposed but are involved in hydrogen-bonding interactions with other amino acids, and the hydrophobic core around the D helix, whose packing rearrangement provides the driving force in the sorcin signal transmission pathway, is conserved.

At this point it appears useful to speculate on the mechanism used by PEF proteins to amplify the small Ca^{2+}-induced conformational changes just discussed that occur in the Ca^{2+} binding domain to achieve target protein interaction. This requires exposure of hydrophobic patches resulting from the movement of the N- and C-terminal domains relative to each other (12). Interestingly, the loop connecting EF3 to EF4 contains a stretch of conserved residues, GFRL in sorcin and GYRL in ALG-2, that were proposed to interact with the N-terminal domain in the Ca^{2+}-free state and to become solvent-exposed upon Ca^{2+} binding (12, 14). One may speculate that these conserved residues play a role in the amplification of the Ca^{2+} signal by transmitting the conformational change to the N-terminal domain, and this may be the reason for the sequence conservation.

In conclusion, the unusual functional coupling operative in sorcin appears applicable to all PEF proteins. It may be envisaged that their activation mechanism depends on subtle changes in the packing of hydrophobic residues located around the D helix that links the site endowed with the highest affinity for Ca^{2+} to the rest of the molecule.

REFERENCES

1. Blanchard, H., Grochulski, P., Li, Y., Arthur, S. C., Davies, P. L., Elce, J. S., and Cygler, M. (1997) *Nat. Struct. Biol.* **4,** 532–538
2. Lin, G., Chattopadhyay, D., Maki, M., Wang, K. K. W., Carson, M., Jin, L., Yu, P. W., Takano, E., Hatanaka, M., DeLucas, L. J., and Narayana, S. V. (1997) *Nat. Struct. Biol.* **4,** 539–546
3. Lollike, K., Johnsen, A. H., Durussel, I., Borregaard, N., and Cox, A. (2001) *J. Biol. Chem.* **276,** 17762–17769
4. Lo, K. W.-H., Zhang, Q., Li, M., and Zhang M. (1999) *Biochemistry* **38,** 7498–7508
5. Kitaura, Y., Watanabe, M., Satoh, H., Kawai, T., Hitomi, K., and Maki, M. (1999) *Biochem. Biophys. Res. Commun.* **263,** 68–75
6. Meyers, M. B., Puri, T. S., Chien, A. J., Gao, T., Hsu, P. H., Hosey, M. M., and Fishman, G. I. (1998) *J. Biol. Chem.* **273,** 18930–18935
7. Meyers, M. B., Pickel, V. M., Sheu, S. S., Sharma, V. K., Scotto, K. W., and Fishman, G. I. (1995) *J. Biol. Chem.* **270,** 26411–26418
8. Pack-Chung, E., Meyers, M. B., Pettingell, W. P., Moir, R. D., Brownawell, A. M., Cheng, I., Tanzi, R. E., and Kim, T. W. (2000) *J. Biol. Chem.* **275,** 14440–14445
9. Brownawell, A. M., and Creutz, C. E. (1997) *J. Biol. Chem.* **272,** 22182–22190
10. Clemen, C. S., Hofmann, A., Zamparelli, C., and Noegel, A. A. (1999) *J. Muscle Res. Cell Motil.* **20,** 669–679
11. Salzer, U., Hinterdorfer, P., Hunger, U., Borken, C., and Prohaska, R. (2002) *Blood* **99,** 2569–2577
12. Ilari, A., Johnson, K. A., Nastopoulos, V., Verzili, D., Zamparelli, C., Colotti, G., Tsernoglou, D., and Chiancone, E. (2002) *J. Mol. Biol.* **317,** 447–458
13. Jia, J., Han, Q., Borregaard, N., Lollike, K., and Cygler, M. (2000) *J. Mol. Biol.* **300,** 1271–1281
14. Jia, J., Tarabykina, S., Hansen, C., Berchtold, M., and Cygler, M. (2001) *Structure (Lond.)* **9,** 267–275
15. Xie, X., Dwyer, M. D., Swenson, L., Parker, M. H., and Botfield, M. C. (2001) *Protein Sci.* **10,** 2419–2425
16. Jia J., Borregaard, N., Lollike, K., and Cygler, M. (2001) *Acta Crystallogr. Sect. D* **57,** 1843–1849
17. Strobl, S., Fernandez-Catalan, C., Braun, M., Huber, R., Masumoto, H., Nakagawa, K., Irie, A., Sorimachi, H., Bourenkow, G., Bartunik, H., Suzuki, K., and Bode, W. (2000) *Proc. Natl. Acad. Sci. U. S. A.* **97,** 588–592
18. Hosfield, C. M., Elce, J. S., Davies, L., and Jia, Z. (1999) *EMBO J.* **18,** 6880–6889
19. Zamparelli, C., Ilari, A., Verzili, D., Giangiacomo, L., Colotti, G., Pascarella, S., and Chiancone, E. (2000) *Biochemistry* **39,** 658–666
20. Kitaura, Y., Matsumoto, S., Satoh, H., Hitomi, K., and Maki, M. (2001) *J. Biol. Chem.* **276,** 14053–14058
21. Meyers, M. B., Zamparelli, C., Verzili, D., Dicker, A. P., Blanck, T. J. J., and Chiancone, E. (1995) *FEBS Lett.* **357,** 230–234
22. Zamparelli, C., Ilari, A., Verzili, D., Vecchini, P., and Chiancone, E. (1997) *FEBS Lett.* **1,** 1–6
23. Verzili, D., Zamparelli, C., Mattei, B., Noegel, A. A., and Chiancone, E. (2000) *FEBS Lett.* **471,** 197–200
24. Higuchi, R., Krummel, B., and Saiki, R. K. (1988) *Nucleic Acids Res.* **16,** 7351–7367
25. Chou, P. Y., and Fasman, G. D. (1974) *Biochemistry* **13,** 222–224
26. Bryant, D. T. W. (1985) *Biochem. J.* **226,** 613–616
27. André, I., and Linse, S. (2002) *Anal. Biochem.* **305,** 195–205
28. Laemmli, U. K. (1970) *Nature* **227,** 680–685
29. Towbin, H., Staehelin, T., and Gordon, J. (1979) *Proc. Natl. Acad. Sci. U. S. A.* **76,** 4350–4354
30. Bjellqvist, B., Hughes, G. J., Pasquali, Ch., Paquet, N., Ravier, F., Sanchez, J.-C., Frutiger, S., and Hochstrasser, D. F. (1993) *Electrophoresis* **14,** 1023–1031
31. Tsien, R. Y., and Pozzan, T. (1989) *Methods Enzymol.* **172,** 230–262
32. Nelson, M. R., and Chazin, W. J. (1998) *Biometals* **11,** 297–318
33. Glaser, F., Pupko, T., Paz, I., Bell, R. E., Bechor-Shental, D., Martz, E., and Ben-Tal, N. (2003) *Bioinformatics* **19,** 163–164
34. Jaren, O. R., Harmon, S., Chen, A. F., and Shea, M. A. (2000) *Biochemistry* **39,** 6881–6890
35. Fefeu, S., Biekofsky, R. R., McCormick, J. E., Martin, S. R., Bayley, P. M., and Feeney, J. (2000) *Biochemistry* **39,** 15920–15931
36. Dutt, P., Arthur, J. S. C., Grochulski, P., Cygler, M., and Elce, J. S. (2000) *Biochem. J.* **348,** 37–43
37. Strickland, E. H. (1974) *CRC Crit. Rev. Biochem.* **2,** 113–175
38. Sun, H., Yin, D., Coffeen, L. A., Shea, M. A., and Squier, T. C. (2001) *Biochemistry* **40,** 9605–9617
39. Kraulis, P. J. (1993) *J. Appl. Crystallogr.* **26,** 283–291
40. Biacore AB (1994) *BIAtechnology Handbook*, Version AB, pp. 4–5, Biacore AB, Uppsala, Sweden

Information Transfer in the Penta-EF-hand Protein Sorcin Does Not Operate via the Canonical Structural/Functional Pairing: A STUDY WITH SITE-SPECIFIC MUTANTS

Manuela Mella, Gianni Colotti, Carlotta Zamparelli, Daniela Verzili, Andrea Ilari and Emilia Chiancone

Access the most updated version of this article at doi: 10.1074/jbc.M213276200

Alerts:
- When this article is cited
- When a correction for this article is posted

Click here to choose from all of JBC's e-mail alerts

This article cites 39 references, 12 of which can be accessed free at
http://www.jbc.org/content/278/27/24921.full.html#ref-list-1